

Reversible Adsorption on a Random Site Surface

C. Oleyar and J. Talbot

*Department of Chemistry and Biochemistry, Duquesne University, Pittsburgh, PA
15282-1530, USA*

Abstract

We examine the reversible adsorption of hard spheres on a random site surface in which the adsorption sites are uniformly and randomly distributed on a plane. Each site can be occupied by one solute provided that the nearest occupied site is at least one diameter away. We use a numerical method to obtain the adsorption isotherm, i.e. the number of adsorbed particles as a function of the bulk activity. The maximum coverage is obtained in the limit of infinite activity and is known exactly in the limits of low and high site density. An approximate theory for the adsorption isotherms, valid at low site density, is developed by using a cluster expansion of the grand canonical partition function. This requires as input the number of clusters of adsorption site of a given size. The theory is accurate for the entire range of activity as long as the site density is less than about 0.3 sites per particle area. We also discuss a connection between this model and the vertex cover problem.

Key words: Adsorption; random site surface; cluster expansion; vertex cover
PACS: 05.70.Np, 05.20.-g,

1 Introduction

The adsorption of proteins and colloids at a liquid-solid interface is a key step in many natural and industrial processes such as filtration, chromatography, protein purification, immunological assays, biosensors, biomineralization and biofouling. In many of these situations, the surface of the adsorbent is heterogeneous. For example, in immunological assays one typically employs colloidal particles that have been coated with proteins (antibodies) to bind with antigens that may be present in the sample. Similarly, in affinity chromatography, the adsorbent is synthesized by immobilizing certain affinity ligands on porous silica, agarose or synthetic polymers. Many of these applications can benefit from a quantitative knowledge of the amount of solute that is adsorbed as a

function of the bulk concentration, ligand density and distribution and solute properties such as the size.

The modeling approach required depends on the nature of the adsorption. When there is a finite desorption probability, characterized by a non-zero desorption rate constant, an equilibrium between the bulk and adsorbed phases will be established; rapidly if the desorption rate is large and more slowly for small desorption rates. The properties of the equilibrium state, in particular the adsorption isotherm, depend on the bulk phase activity. If the desorption rate constant is very small on the experimental time scale the adsorption is effectively irreversible and a different approach is required.

The statistical mechanics of reversible adsorption on heterogeneous surfaces, particularly for gases on solids, has a long history. Pioneering work was performed by Hill (1) and Steele (2) and it is still an active area of research (3; 4). There is also a well-developed literature on irreversible adsorption on homogeneous surfaces (5; 6; 7). Some models specifically address irreversible adsorption on non-uniform surfaces (8; 9; 10; 11) where macromolecules are represented as hard spheres that bind irreversibly to adsorption sites. In the simplest of these, the Random Site Surface (RSS) (8), the sites are represented by randomly distributed points. Adamczyk et al (10) extended the basic model to the situation where the adsorption sites have finite dimensions. The adsorption of colloidal (12; 13) and nanoparticles (14) has been interpreted with these models and a similar hard sphere model was used to rationalize the adsorption of proteins to hydrophobic sites on mixed self-assembled monolayers (15).

Although macromolecules such as colloids and proteins have a tendency to adsorb irreversibly, this is not always the case and it is certainly useful to understand the equilibrium behavior. In this article we therefore present numerical and approximate analytical results for reversible adsorption of hard spheres on the RSS. For irreversible adsorption on this surface the task of developing a theoretical description was greatly simplified by the existence of an exact mapping to an analogous process on a continuous (homogeneous) surface (8). For reversible adsorption on the RSS surface, however, there appears to be no similar mapping that would allow us to exploit the known behavior of hard spheres on continuous surfaces (16; 17).

In addition to its application to adsorption, the RSS model is also interesting from another perspective. Weight and Hartmann obtained analytical results for the minimal vertex cover on a random graph by a mapping to a hard sphere lattice gas (18; 19). A vertex cover of an undirected graph is a subset of the vertices of the graph which contains at least one of the two endpoints of each edge. In the vertex cover problem one seeks the *minimal vertex cover* or the vertex cover of minimum size of the graph. This is an NP-complete problem meaning that it is unlikely that there is an efficient algorithm to solve it.

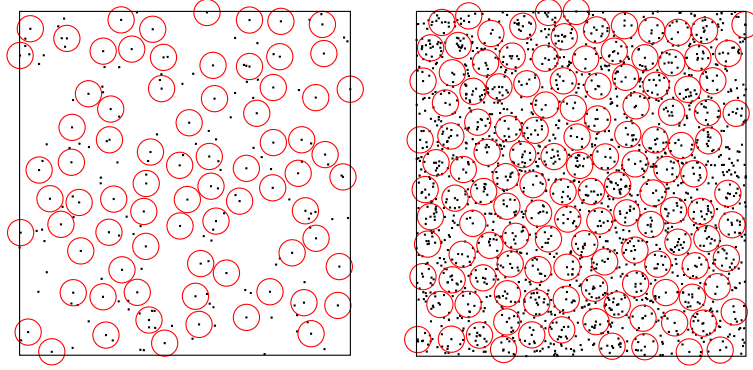


Fig. 1. Sample configurations of adsorbed hard spheres on the random site surface. A sphere may bind, centered, to a site as long as the nearest occupied site is at least σ away. Left configuration: $\alpha = 1, N_s = 200, \theta = 0.380$; right configuration: $\alpha = 10, N_s = 2000, \theta = 0.650$. In both cases $\lambda = 10000$.

The connection to the adsorption model is made by associating a vertex with each adsorption site. An edge is present between any two vertices (or sites) if they are closer than the adsorbing particle diameter. The minimal vertex cover corresponds to densest particle packings. Weight and Hartmann obtained an analytical solution for the densest packing of hard spheres on random graph using a replica-symmetric approach. Although the random graph is related to the RSS model, it is not the same as the former does not have a physical structure. Specifically, in a random graph each possible edge is present with a given probability, c . In the random site surface, on the other hand, two adsorption sites that are neighbors of a given site are more likely to be neighbors of each other than two randomly selected sites. This effect can be quantified by the clustering coefficient, which is the average probability that two neighbors of a given vertex are also neighbors of one another.

In section 2 we define the model and the simulation procedure. Section 3 compares numerical results for the maximum coverage with various theoretical estimates. The structure of the random site surface is discussed in section 4, and section 5 presents an approximate theory for the adsorption isotherms that applies at low adsorption site density.

2 Model and Simulation

The adsorbent surface consists of N_s point sites that have been uniformly and randomly distributed on a surface of area L^2 . These sites are frozen in place. The adsorbate molecules are represented by hard spheres of diameter σ . In order to adsorb, a hard sphere must bind, centered, to one site. An adsorbed sphere may cover any number of sites but only occupies (or interacts with) the one at its center. Any site that lies within a distance σ of an occupied site

is unavailable. See Figure 1. It is convenient to introduce a dimensionless site density

$$\alpha = \frac{\pi\sigma^2 N_s}{4L^2} \quad (1)$$

corresponding to the average number of sites in an area equal to the projected area of a sphere. The coverage is defined as

$$\theta = \frac{\pi\sigma^2 n}{4L^2}, \quad (2)$$

where n is the number of adsorbed spheres. If the adsorption is irreversible it was shown in Ref (8) that the coverage at time t is equal to the coverage on a continuous surface at time τ ,

$$\theta(t; \alpha) = \theta_c(\tau), \quad (3)$$

where τ and t are related by

$$\tau = \alpha(1 - e^{-t/\alpha}), \quad (4)$$

which has the required property that as $\alpha \rightarrow \infty$, $\tau \rightarrow t$. Although the time-dependent coverage on the continuous surface $\theta_c(\tau)$, is itself not known exactly, semi-empirical equations that provide an accurate representation of numerical simulations of the model have been proposed (8). It is not clear, however, how to develop a similar mapping to apply to the reversible (equilibrium) case.

In the reversible binding case there is an equilibrium between a bulk phase containing adsorbate at activity λ , and the thermodynamic properties of the adsorbed phase can be obtained from the grand canonical partition function. For a particular realization of the adsorption site distribution this is:

$$\Xi(\lambda, N_s) = \sum_{n_i=0,1} \left[\prod_{i>j} (1 - f_{ij} n_i n_j) \prod_i \lambda^{n_i} \right], \quad (5)$$

where $\lambda = \exp(\beta\mu)$ is the activity with $\beta = 1/k_B T$ and μ is the chemical potential. Site i is occupied (vacant) if $n_i = 1(0)$ and $f_{ij} = 1$ if sites i and j are closer than σ and zero otherwise.

The number of adsorbed molecules can be computed directly from the partition function:

$$\langle n \rangle = \lambda \left(\frac{\partial \ln \Xi}{\partial \lambda} \right)_{N_s} \quad (6)$$

as can the fluctuation in the adsorbed number:

$$\langle (\delta n)^2 \rangle = \lambda \left(\frac{\partial \langle n \rangle}{\partial \lambda} \right)_{N_s} \quad (7)$$

It is generally not possible to evaluate this partition function analytically, even in one-dimension. However, if all the sites are isolated $f_{ij} = 0, \forall i, j$ the partition function becomes

$$\Xi(\lambda, N_s) = (1 + \lambda)^{N_s}, \quad (8)$$

which yields the Langmuir form for the fraction of occupied sites,

$$\theta = \alpha \frac{\lambda}{1 + \lambda} \quad (9)$$

and fluctuation

$$\langle (\delta n)^2 \rangle = N_s \frac{\lambda}{(1 + \lambda)^2}. \quad (10)$$

We have used a Gillespie type algorithm (20; 21) to obtain the adsorption isotherms of the RSS model numerically. First, N_s sites are distributed uniformly and randomly in a periodic unit cell. A list of the neighbors, i.e. those that lie within a distance σ , of each site is then constructed. At each step of the simulation, the total event rate is $R = \phi + n/\lambda$ where ϕ is the fraction of sites that are available, and n is the number of occupied sites. A waiting time is generated from an exponential distribution using $t = -\ln(\xi)/R$ where ξ is a uniform random number. A second random number is used to decide the type of event. If $\xi < \phi/(\phi + n/\lambda)$ a new sphere is added to the surface at an available site selected at random. Otherwise, one of the spheres on the surface is removed. For a given value of λ , the adsorption/desorption process is allowed to continue until the system reaches a steady state and then the number of adsorbed spheres is averaged over a large number of events (typically one million). In the steady state this procedure is equivalent to a grand canonical Monte Carlo simulation.

All of the simulation results reported here were obtained using 4000 adsorption sites. Several tests were performed with larger and smaller systems, but there was no noticeable system size effect. Up to 20 different realizations of the adsorption sites were used. The isotherms were generated by performing a series of simulations with increasing activity in the interval $\lambda_{\min} \leq \lambda \leq \lambda_{\max}$. The final configuration of a simulation at given activity served as the initial configuration for the following simulation at higher activity. For each value of the activity n_{trial} events were simulated. In order to allow the system to equilibrate at each new activity, only the second half of the n_{trial} events were used in the calculation of the ensemble averages.

The activity schedule was determined from the formula:

$$\lambda_i = \lambda_{\min} \left(\frac{\lambda_{\max}}{\lambda_{\min}} \right)^{\frac{i}{n_\lambda - 1}}, \quad i = 0, \dots, n_\lambda - 1 \quad (11)$$

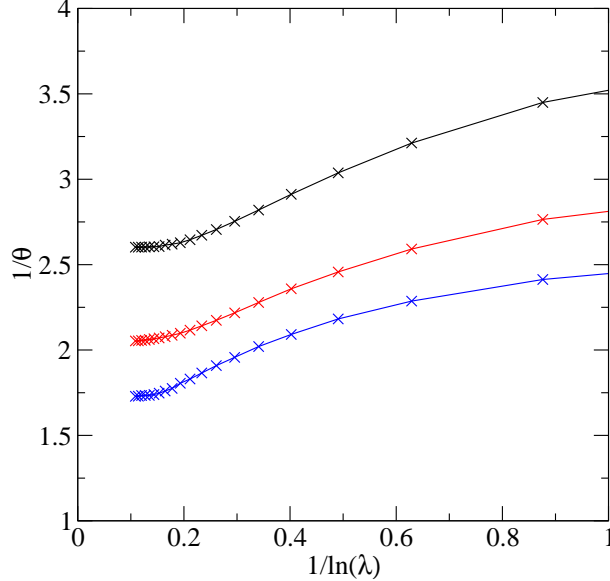


Fig. 2. Adsorption Isotherms from simulation. Results are averages over 20 realizations of 4000 sites. $\alpha = 1, 2, 4$ top to bottom.

For the adsorption isotherms at low activities we used $\lambda_{\min} = 0.1$, $\lambda_{\max} = 100$ and $n_{\lambda} = 20$ and $n_{\text{trial}} = 50000$.

As long as the activity is not too large, or whenever $\alpha \leq 0.8$, the simulations are non-problematic in that the steady state is reached rapidly and reproducibly. For larger values of *alpha* at high activities, some care is needed to ensure that the system reaches equilibrium. The parameters n_{λ} and n_{trial} were increased until further changes had no influence of the isotherms. In most cases, $n_{\lambda} = 50$ and $n_{\text{trial}} = 5 \times 10^5$ were sufficient.

Although we did not employ the method in this study, parallel tempering (22; 23) would be an alternative, and possibly more efficient, method at large values of the activity.

3 Maximum Coverage

The maximum coverage is obtained in the limit $\lambda \rightarrow \infty$. As the site density approaches zero, all sites become independent and the maximum coverage is α . In the limit $\alpha \rightarrow \infty$ the surface becomes smooth and an adsorbing sphere can occupy any position. The densest configuration in this case corresponds to a hexagonal close packing of spheres with a coverage of $\theta_{\text{hcp}} = \pi/(2\sqrt{3}) = 0.90687\dots$ (24).

To obtain numerical values between these two limits for a given value of α we performed simulations using $\lambda_{\min} = 10$, $\lambda_{\max} = 100000$ and $n_{\lambda} = 50$. Some

sample isotherms, showing $1/\theta$ versus $1/\lambda$, are shown in Figure 2. When $1/\lambda$ is sufficiently small, the curve approaches a plateau. These maximum values for different α are presented in Fig 3 together with various theories including the Langmuir approximation, the cluster theory to second order (see section 5) and the maximum coverage in an irreversible adsorption process (the “jamming limit”) (8).

Weight and Hartmann (18; 19) used a statistical mechanics approach to the minimum vertex cover problem on a finite connectivity random graph. By using a replica-symmetric approach, they showed that the average maximum fraction of occupied graph vertices is

$$\nu_{\max} = \frac{2W(c) + W(c)^2}{2c}, \quad (12)$$

where $W(x)$ is the Lambert-W function defined by $W(x)e^{W(x)} = x$ and c is the average connectivity of the random graph. From Eq 1 and Eq 2 it is easy to show that $\nu = N/N_s = \theta/\alpha$. Finally, in order to connect c to α we note that in a random graph, the distribution of connectivities is given by a Poisson distribution with mean c . Therefore, the probability that a vertex has a connectivity of zero is $\exp(-c)$. Similarly, for a random distribution of points in the plane at a density α the probability that a point has no neighbors (closer than σ) is $\exp(-4\alpha)$ (c.f. Eq 15). Therefore, we take $c = 4\alpha$. Substituting these results in Eq 12, the maximum coverage on a random graph is

$$\theta_{\max} = \frac{1}{4}W(4\alpha) + \frac{1}{8}W(4\alpha)^2. \quad (13)$$

It is evident that the Langmuir approximation of independent sites is very poor, even for quite small values of α . As expected, due to the inherent inefficiency of irreversible adsorption, the RSA coverage underestimates the maximum coverage for all values of α . The remaining theories, all of which are equilibrium, consistently overestimate the maximum coverage. The cluster theory to second order provides a good estimate up to $\alpha \approx 0.3$

4 Structure of the random site surface

The connectedness of the adsorption sites is a strong function of the dimensionless site density, as can be seen in Fig. 4. For a given distribution of sites, increasing this parameter corresponds to increasing the size of the adsorbing spheres. At small values of α , the surface consists of isolated clusters of sites. A cluster consists of n sites all of which are closer than σ to at least one other site of the cluster. For small values of α the majority of sites are isolated. Above

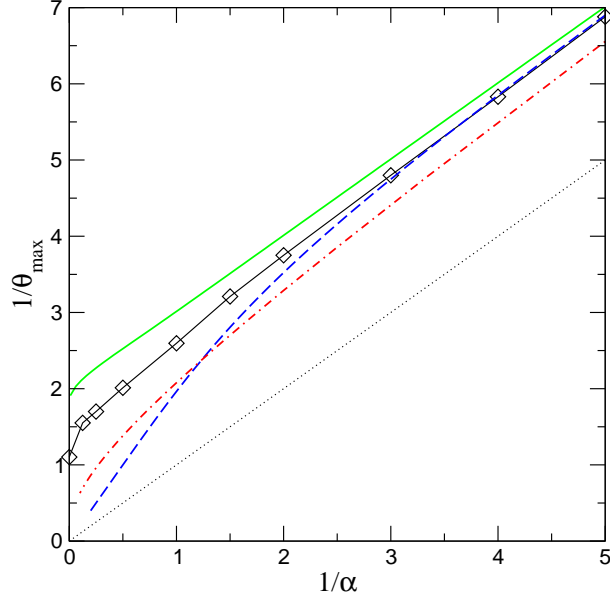


Fig. 3. Maximum Coverage as a function of the inverse site density. Squares: numerical simulation; upper solid line: irreversible adsorption; dashed line: cluster theory to second order; dash-dotted line: random graph; dotted line: independent site assumption.

a certain value of $\alpha_c \approx 0.8$ percolation occurs and almost all sites belong to a giant cluster (25).

In order to develop an approximate theory for the adsorption isotherms, we need to know the expected number of clusters of given type as a function of the site density. Analytical expressions for isolated sites and pairs can be obtained by making use of the following well-known result. Consider a region of area A that contains a finite number N of sites at given positions. The probability that none of the remaining $N_s - N$ points lies in this region (in the large N_s limit) is

$$p_0 = e^{-\rho_s A}. \quad (14)$$

where $\rho_s = N_s/L^2$ is the site density. A given site is isolated if there are no other sites within a circle of radius σ centered on the given site. Therefore the expected number of isolated sites (per adsorption site) is

$$x_1 = e^{-4\alpha}. \quad (15)$$

The number of pairs of sites that are separated by a distance between r and $r + dr$ is $\frac{1}{2}2\pi r\rho_s dr$. Now imagine two circles of radius σ centered on these sites. Let $A_2(r)$ represent the area of union of these two circles. If any other site lies within this area, the two sites do not form a pair. The probability that no other site lies within this area is $\exp(-A_2(r)\rho_s)$ where of diameter σ separated by r . So the probability that two sites separated by r form a pair is $\rho_s \pi r \exp(-A_2(r)\rho_s) dr$. Integrating over r and introducing the dimensionless

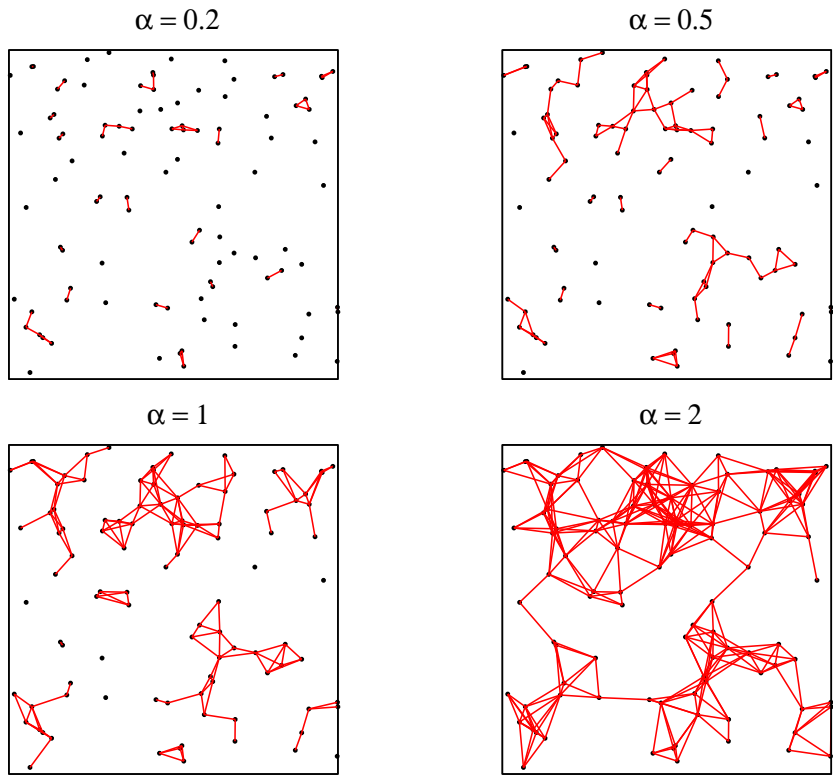


Fig. 4. Structure of the random site surface for different values of α . Two sites are connected if they are closer than σ .

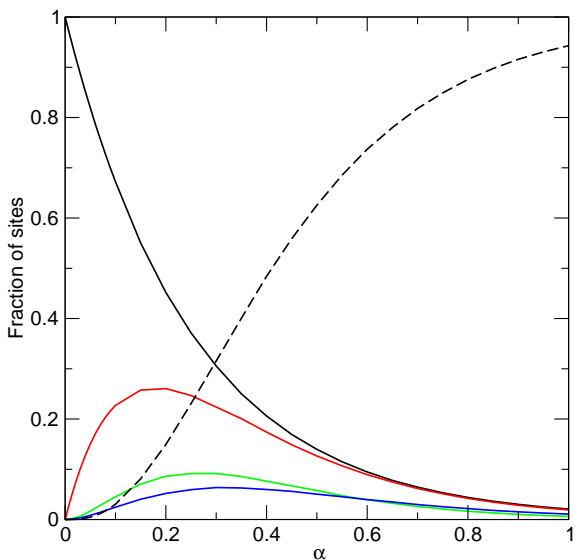


Fig. 5. Fraction of sites belonging to clusters of various sizes. From top to bottom, left hand side: isolated sites, pairs, triplets type a; triplets type b. The dashed line shows the fraction of sites not belonging to any of these types

variables α and $y = r/\sigma$ leads to the final expression for the number of pairs:

$$x_2 = 4\alpha \int_0^1 \exp\left[-\frac{4\alpha}{\pi} A_2(y)\right] y dy, \quad (16)$$

where $A_2(y) = 2(\pi - \cos^{-1}(y/2)) - y\sqrt{1 - y^2/4}$. Although this integral cannot be expressed in terms of elementary functions, it is straightforward to calculate numerically. A similar procedure could obviously be used to evaluate the expected number of higher order clusters, although the task rapidly becomes cumbersome.

Numerical results for isolated sites, and clusters composed of two and three sites are presented in Fig 5. These were obtained by averaging over 100 independent distributions of 4000 sites each in a square cell with periodic boundary conditions. The theoretical expression, Eq 16 is indistinguishable from the numerical results.

For $\alpha \leq 0.1$ the surface consists almost entirely of isolated sites and pairs, while for $\alpha = 0.5$ about 50% of the sites belong to clusters of cardinality four or greater. For convenience, we also fitted the numerical results using simple functions. For pairs the numerical data is very well fitted by the equation:

$$x_2 = 2\alpha \exp(-5.578\alpha), \quad 0 \leq \alpha \leq 1. \quad (17)$$

There are two kinds of triplets. In type “3a” two sites are neighbors of a third site but not of each other, while in type “3b” each site is a neighbor of the other two. The number of each kind is well described by

$$x_{3a} = 3.249\alpha^2 \exp(-7.537\alpha), \quad 0 \leq \alpha \leq 1 \quad (18)$$

and

$$x_{3b} = 1.519\alpha^2 \exp(-6.250\alpha), \quad 0 \leq \alpha \leq 1. \quad (19)$$

As can be seen in Fig 6, these fitting functions provide an excellent approximation of the numerical results.

5 Approximate theory for the adsorption isotherms at low site density

Assuming that the adsorption surface consists of isolated clusters of sites, the partition function may be expressed as

$$\Xi = (\Xi_1)^{N_1} (\Xi_2)^{N_2} (\Xi_{3a})^{N_{3a}} (\Xi_{3b})^{N_{3b}} \dots, \quad (20)$$

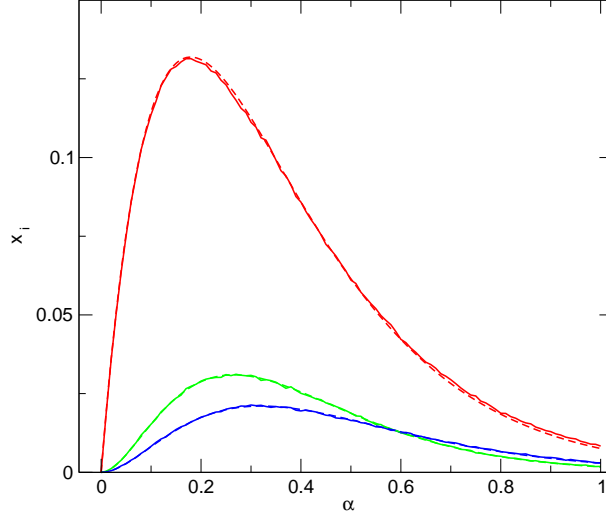


Fig. 6. Fraction of pairs, and triplets of type 3a and 3b (top to bottom left hand side) as a function of the dimensionless site density from numerical simulation. The fitting functions Eqs 17,18, and 19 are shown as dashed lines.

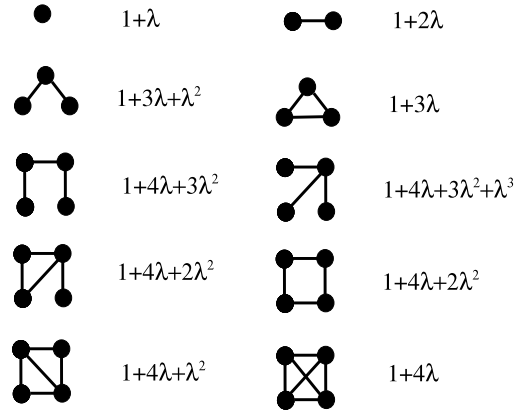


Fig. 7. Clusters with grand canonical partition function. A solid line connects two sites that are closer than σ . Triplets of type “3a” and “3b” are shown left to right in the second row.

where $N_i = x_i N_s$ is the number of clusters of type i . This factorization is possible because adsorption on a given cluster does not affect any of the others. The adsorption isotherm is, from Eq. 6,

$$\langle n \rangle = \lambda N_1 \left(\frac{\partial \ln \Xi_1}{\partial \lambda} \right) + \lambda N_2 \left(\frac{\partial \ln \Xi_2}{\partial \lambda} \right) + \dots \quad (21)$$

Figure 7 shows the first few possible clusters and the associated grand canonical ensemble partition function. A solid line connecting two sites indicates that they are closer than a particle diameter and therefore cannot be simultaneously occupied. The partition function is evaluated by explicit summation

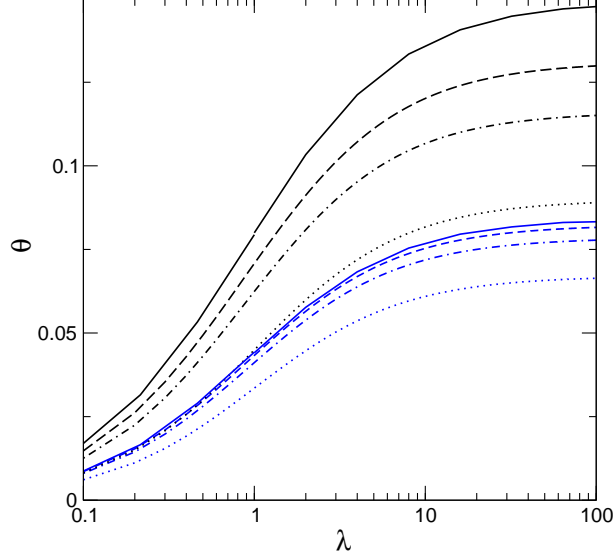


Fig. 8. Isotherms for $\alpha = 0.2, 0.1$, top to bottom. The solid lines show simulation results (an average of 10 distributions of 4000 sites). The dotted, dash-dotted and dashed lines show the cluster expansion to first (x_1), second (x_2) and third order ($x_{3a} + x_{3b}$), respectively.

over all sites. As an example, for the first of the two triplets,

$$\Xi_{3a} = \sum_{n_1=0}^1 \sum_{n_2=0}^1 \sum_{n_3=0}^1 (1 - n_1 n_2)(1 - n_1 n_3) \lambda^{n_1+n_2+n_3} = 1 + 3\lambda + \lambda^2. \quad (22)$$

By substituting these results into Eq 21 we obtain

$$\theta = \alpha \left[\frac{\lambda}{1+\lambda} x_1 + \frac{2\lambda}{1+2\lambda} x_2 + \frac{3\lambda + 2\lambda^2}{1+3\lambda + \lambda^2} x_{3a} + \frac{3\lambda}{1+3\lambda} x_{3b} + \dots \right] \quad (23)$$

We show the predictions of this equation to different orders compared with the simulation results in Fig 8. Successive approximations approach the simulated isotherm from below. Including clusters up to triplets described the numerical simulation data accurately for $\alpha = 0.1$, but is already quite poor for $\alpha = 0.2$. This rapid breakdown can be understood by realizing that truncation of the expansion means that one is failing to include all sites.

An alternative approach is to assume that all sites belong to clusters up to a given order. Thus, if all sites are assumed to be isolated we have

$$\Xi = \Xi_1^{N_s} = (1 + \lambda)^{N_s}, \quad (24)$$

which gives for the coverage the Langmuir expression:

$$\theta_1 = \alpha \frac{\lambda}{1 + \lambda}. \quad (25)$$

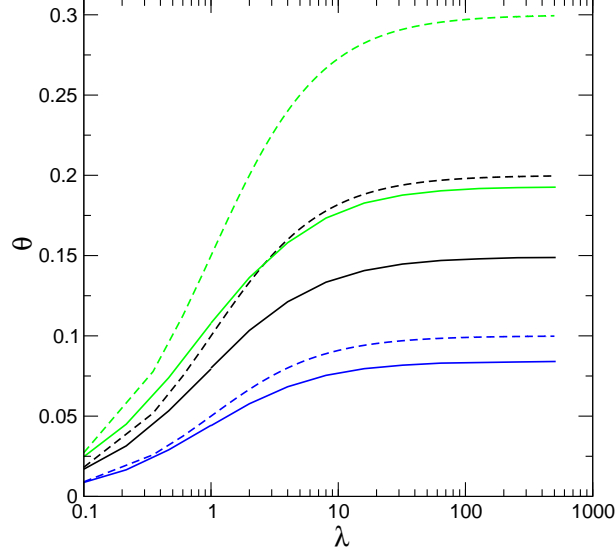


Fig. 9. Isotherms for $\alpha = 0.3, 0.2, 0.1$, top to bottom. Solid and dashed lines show the simulation results and the Langmuir theory, respectively.

For $\lambda \rightarrow \infty$ this gives $\theta_1 = \alpha$, i.e. all sites are occupied. When it is assumed that only isolated sites and sites with one neighbor are present, the number of the latter is estimated as $N_2 = (N_s - N_1)/2 = N_s(1 - \exp(-4\alpha))/2$. The partition function is

$$\Xi = \Xi_1^{N_1} \Xi_2^{N_2} = (1 + \lambda)^{N_1} (1 + 2\lambda)^{N_2}, \quad (26)$$

which leads to a coverage of

$$\theta_2 = \frac{\alpha}{N_s} \left(\frac{N_1 \lambda}{1 + \lambda} + \frac{2N_2 \lambda}{1 + 2\lambda} \right) = \alpha \lambda \frac{1 + \lambda(1 + \exp(-4\alpha))}{(1 + 2\lambda)(1 + \lambda)}. \quad (27)$$

The maximum coverage at this level of approximation, obtained by taking the limit $\lambda \rightarrow \infty$, is

$$\theta_{2,\max} = \frac{\alpha}{2} (1 + \exp(-4\alpha)) = \alpha - 2\alpha^2 + O(\alpha^3). \quad (28)$$

At the triplet level, we estimate the total number of triplets as $N_3 = (N_s - N_1 - 2N_2)/3$. Of these, a fraction $y_{3a} = x_{3a}/(x_{3a} + x_{3b})$ are of type a and the remainder are of type b. This yields:

$$\theta_3 = \alpha \left[\left(y_{3b} \frac{3\lambda}{1 + 3\lambda} + y_{3a} \frac{3\lambda + 2\lambda^2}{1 + 3\lambda + \lambda^2} \right) \frac{1 - x_1 - 2x_2}{3} + \frac{2\lambda}{1 + 2\lambda} x_2 + \frac{\lambda}{1 + \lambda} x_1 \right]. \quad (29)$$

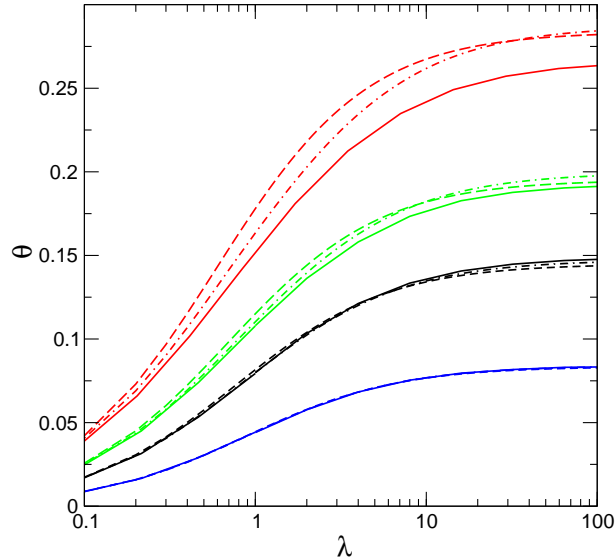


Fig. 10. Isotherms for $\alpha = 0.5, 0.3, 0.2, 0.1$, top-to-bottom. The solid lines show the simulation results, while the dashed and dash-dot lines show the approximate theories θ_2 and θ_3 , respectively

The maximum coverage is then:

$$\theta_{3,\max} = \alpha[(y_{3a} + 1)(1 - x_1 - 2x_2)/3 + x_2 + x_1]. \quad (30)$$

Figures 9 and 10 show the simulated isotherms compared with the alternative theory. Unlike the theoretical estimates shown in Fig 8, the estimates generally lie above the simulation results. It is clear that the Langmuir model (all sites assumed to be isolated) provides a very poor description, even at quite low site densities. There is not much difference between the second and third order cluster expansions. Both provide a satisfactory description of the isotherm for $\alpha \leq 0.3$.

6 Conclusion

We have obtained numerical results for the isotherms of hard spheres adsorbing on a random site surface. For a given configuration of sites the maximum coverage is obtained by taking the limit of infinite bulk phase activity. We developed an approximate theory based on a cluster expansion of the partition function that is accurate up to moderate site density.

Weight and Hartmann obtained an analytic solution for a related model of hard spheres on a random graph using replica theory. Their solution applies only to the densest particle packing. Generalization of their approach to finite activity or to the RSS surface does not appear to be straightforward. Perhaps

an alternative approach will allow a description of the thermodynamics for a wider range of site densities than is possible using the theory proposed here.

Acknowledgments

We thank David Dean, Gilles Tarjus and Pascal Viot for useful discussions.

References

- [1] T. L. Hill, Statistical mechanics of adsorption. vi. localized unimolecular adsorption on a heterogeneous surface, *J. Chem. Phys.* 17 (1949) 762.
- [2] W. A. Steele, Monolayer adsorption with lateral interaction on heterogeneous surfaces, *J. Chem. Phys.* 67 (1963) 2016.
- [3] W. Rudzinski, D. H. Everett, *Adsorption of Gases on Heterogeneous Surfaces*, Academic Press, 1992.
- [4] W. Steele, The supersite approach to adsorption on heterogeneous surfaces, *Langmuir* 15 (1999) 6083.
- [5] J. W. Evans, Random and cooperative sequential adsorption, *Rev. Mod. Phys.* 65 (1993) 1281.
- [6] J. Talbot, G. Tarjus, P. R. V. Tassel, P. Viot, From car parking to protein adsorption: A review of sequential addition processes, *Colloids and Surfaces A* 165 (2000) 287.
- [7] P. Schaaf, J.-C. Voegel, B. Senger, From random sequential adsorption to ballistic deposition: A general view of irreversible deposition processes, *J. Phys. Chem. B* 104 (2000) 2204.
- [8] X. Jin, N. H. L. Wang, G. Tarjus, J. Talbot, Irreversible adsorption on non-uniform surfaces: the random site model, *J. Phys. Chem.* 97 (1993) 4256.
- [9] X. Jin, J. Talbot, N. H. L. Wang, Analysis of steric hindrance effects on adsorption kinetics and equilibria, *AIChE J.* 40 (1994) 1685.
- [10] Z. Adamczyk, P. Weronki, E. Musial, Irreversible adsorption of hard spheres at random site (heterogeneous) surfaces, *J. Chem. Phys.* 116 (2002) 4665.
- [11] Z. Adamczyk, B. Siwek, P. Weronki, E. Musial, Irreversible adsorption of colloid particles at heterogeneous surfaces, *Applied Surface Science* 196 (2002) 250.
- [12] Y. Lüthi, J. Ricka, M. Borkovec, Colloidal particles at water-glass interface: deposition kinetics and surface heterogeneity, *J. Colloid Int. Sci.* 206 (1998) 314.
- [13] Z. Adamczyk, P. Weronki, E. Musial, Irreversible adsorption of hard spheres at random-site surfaces, *J. Chem. Phys.* 120 (2004) 11155.

- [14] K. D. Kloepper, T.-D. Onuta, D. Amarie, B. Dragnea, Field-induced interfacial properties of gold nanoparticles in ac microelectrophoretic experiments, *J. Phys. Chem. B* 108 (1994) 2547.
- [15] E. Ostuni, B. A. Gryzbowski, M. Mrksich, C. S. Roberts, G. M. Whitesides, Adsorption of proteins to hydrophobic sites on mixed self-assembled monolayers, *Langmuir* 19 (2003) 1861.
- [16] L. Tonks, The complete equation of state of one, two and three-dimensional gases of hard elastic spheres, *Phys. Rev. E* 50 (1936) 955.
- [17] J. Talbot, Molecular thermodynamics of binary mixture adsorption: A scaled particle theory approach, *J. Chem. Phys.* 106 (1997) 4696.
- [18] M. Weight, A. K. Hartmann, Number of guards needed by a museum: A phase transition in vertex covering of random graphs, *Phys. Rev. Lett.* 26 (2000) 6118.
- [19] M. Weight, A. K. Hartmann, Minimal vertex covers on finite-connectivity random graphs: a hard-sphere lattice gas picture, *Phys. Rev. E* 63 (2001) 056127.
- [20] A. B. Bortz, M. H. Kalos, J. L. Lebowitz, A new algorithm for Monte Carlo simulation of Ising spin systems, *J. Compt. Phys.* 17 (1975) 10.
- [21] D. T. Gillespie, Exact stochastic simulation of coupled chemical reactions, *J. Chem. Phys.* 81 (1977) 2340.
- [22] C. J. Geyer, Markov chain Monte Carlo maximum likelihood, in: *Computing and statistics: Proceedings of the 23rd symposium on the interface*, 1991, p. 156.
- [23] D. J. Earl, M. W. Deem, Parallel tempering: Theory, applications, and new perspectives, *Phys. Chem. Chem. Phys.* 7 (2005) 3910.
- [24] L. Fejes Tóth, *Regular Figures*, Macmillan, 1964.
- [25] E. N. Gilbert, Random plane networks, *Journal of the Society for Industrial and Applied Mathematics* 9 (1961) 533.